



STIFFNESS AND DAMPING COEFFICIENTS OF MAGNETO-HYDRODYNAMICS SQUEEZE FILM CHARACTERISTICS FORNON-NEWTONIAN POROUS CURVED CIRCULAR PLATES

Santhana Krishnan Narayanan and Sundarammal Kesavan

Department of Mathematics, SRM University, Kattankulathur, Tamilnadu, India

E-Mail: sundarammal@gmail.com

ABSTRACT

The Stiffness and Damping coefficients of squeeze film dynamic characteristics between porous curved circular plates lubricated with an electrically conducting non-Newtonian fluid in the presence of an external magnetic field are investigated in this paper. The expressions for MHNN porous squeeze film curved circular plate's stiffness and dynamic coefficients are obtained. Comparing with the hydrodynamic Newtonian case, the dynamic stiffness and damping coefficients of squeeze film dynamic characteristics for porous curved circular plates are improved by the use of an electrically conducting non-Newtonian fluid in the presence of external magnetic fields.

Keywords: MHNN characteristics, porous squeeze film, curved circular plates, stiffness coefficients, damping coefficients.

1. INTRODUCTION

Several studies have investigated the MHD effects on the lubrication performances of the journal bearings by Malik and Singh [7], the slider bearings by Lin [6] and squeeze film bearings by Lin *et al* [5]. The presence of additives is found to have beneficial effects on the load-carrying capacity and bearing characteristics by the experimental works by Oliver [9]. Several articles have applied this non-Newtonian (NN) model of couple stress fluids to investigate various squeeze film systems, such as the squeeze film mechanism with reference to human joints by Ahmad and Singh [1] and sphere-plate film by Elsharkasy and AL-Fadhalah [2]. According to their results, the NN influences of couple stresses increase the load-carrying capacity and lengthen the response time for squeeze films. From the above studies, when an electrically conducting fluid is mixed with small amount of long-chained additives, the NN effects of couple stresses would appear in squeeze film. Porous bearing have proved to be useful because of their design simplicity and self-lubricating characteristics. Magneto-hydrodynamic non-Newtonian (MHNN) curved circular squeeze film by Lin *et al* [4]; the curved mechanism is imported for engineering application. Recently, Santhana Krishnan Narayanan and Sundarammal Kesavan[12] have investigated MHNN Squeeze film characteristics of porous curved circular plates.

Therefore, a further investigation is motivated in the present study for porous squeeze film dynamic characteristics in MHNN curved circular plates. The porous squeeze film dynamic characteristics between curved circular plates lubricated with an electrically conducting non-Newtonian fluid in the presence of an external magnetic field are investigated in this paper. The expressions for MHNN porous squeeze film stiffness and dynamic coefficients are obtained. Comparing with the

hydrodynamic Newtonian case, the squeeze film dynamics characteristics for porous curved circular plates are improved by the use of an electrically conducting non-Newtonian fluid in the presence of external magnetic fields.

2. MATHEMATICAL FORMULATION OF THE PROBLEM

As shown in Figure-1 describes the porous squeeze film geometry between upper curved circular plates of radius a approaching the bottom fixed plate of porous bearing of wall thickness H_o with a velocity $\frac{\partial h_c}{\partial t}$ under a constant load.

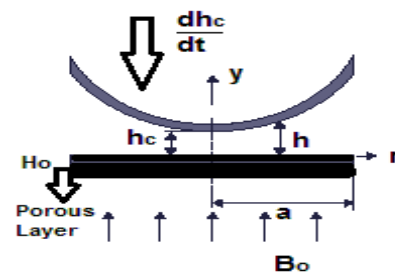


Figure-1. Geometry of MHNN porous squeeze film curved circular plates in the presence of a transverse uniform magnetic field.

The porous region is lubricated with an electrically conducting non-Newtonian couple-stress fluid. An external magnetic field B_o is applied in y -direction.



The film shape h is taken to be an exponential type as Murti [8].

$$h = h_c \exp\left(\frac{-kr^2}{a^2}\right)$$

where h_c is the central minimum film thickness and k is the curved shape parameter. Assume that the thin film lubrication theory as Hamrock[3] is applicable and the induced magnetic field is small when comparing with the magnetic field. Following the MHD flow equation of Lin [6] and the Stokes microcontinuum theory [10], the Magneto-hydrodynamic Non-Newtonian (MHNN) couple stress momentum equations and the continuity equation can be expressed in axially cylindrical coordinates as follows:

$$\frac{\partial p}{\partial r} = \mu \frac{\partial^2 u}{\partial y^2} - \eta \frac{\partial^4 u}{\partial y^4} - \sigma B_o^2 u$$

$$\frac{\partial p}{\partial y} = 0$$

$$\frac{1}{r} \frac{\partial(ru)}{\partial r} + \frac{\partial v}{\partial y} = 0$$

where p is the hydrodynamic film pressure, u and v are the velocity components in the r - and y - directions respectively, μ is the lubricant viscosity, σ denotes the electrical conductivity of the lubricant and η represents a material constant responsible for the non-Newtonian couple stress fluid. The flow of conducting lubricant in the porous region is governed by the modified Darcy's law [11].

$$u^* = -\frac{k'}{\mu} \frac{\partial p^*}{\partial r} \frac{1}{c'^2}$$

$$v^* = -\frac{k'}{\mu(1-\beta)} \frac{\partial p^*}{\partial y}$$

$$\frac{1}{r} \frac{\partial}{\partial r}(ru^*) + \frac{\partial v^*}{\partial y} = 0$$

$$c' = \sqrt{\frac{k' M^2}{m h_{co}^2} - \beta + 1}$$

where p^* is the pressure in the porous matrix, h_{co} denotes the initial minimum film height, k' be the permeability of porous facing, m porosity and β being non dimensional minimum film thickness.

The relevant boundary condition for the velocity components are

$$u = 0, v = 0 \text{ at } y = 0 \quad (6)$$

$$u = 0, v = \frac{\partial h_c}{\partial t} \text{ at } y = h \quad (7)$$

$$\frac{\partial^2 u}{\partial y^2} = 0 \text{ at } y = 0 \text{ \& } y = h \quad (8)$$

The conditions in Eqs (6) and (7) are the conventional non-slip conditions. The condition in Equ (7) comes from the vanishing of couple stresses at the solid boundary[11].

The non-dimensional load-carrying capacity is expressed as

$$W^* = F^* = \frac{Wh_{co}^3}{\mu a^4 \left(-\frac{dh_c}{dt}\right)} = 6\pi \int_{r^*=0}^1 \frac{r^{*3}}{f^*(M, N, h^*)} dr^*$$

where

$$f^*(M, N, h^*) = \frac{12h^*}{M^2} \left\{ 1 - 2 \left[\frac{E_1^3 \tanh\left(\frac{E_2 h^*}{2}\right) + E_2^3 \tanh\left(\frac{E_1 h^*}{2}\right)}{E_1 E_2 (E_1^2 - E_2^2) h^*} \right] \right\}$$

$$M = B_o h_{co} \sqrt{\frac{\sigma}{\mu}}$$

$$l = \sqrt{\frac{\eta}{\mu}}$$

$$N = \frac{l}{h_{co}}$$

$$E_1 = \frac{\sqrt{1 + \sqrt{1 - 4M^2 N^2}}}{\sqrt{2}N}$$

$$E_2 = \frac{\sqrt{1 - \sqrt{1 - 4M^2 N^2}}}{\sqrt{2}N}$$



www.arnjournals.com

$$h^* = \frac{h}{h_{co}} = h_c^* \exp(-kr^{*2})$$

$$r^* = \frac{r}{a}, h_c^* = \frac{h_c}{h_{co}}, p^* = \frac{ph_{co}^3}{\mu a^2 \left(-\frac{dh_c}{dt} \right)}$$

$$V^* = \frac{dh_c^*}{dt} = - \left[6\pi \int_{r^*=0}^1 \frac{r^{*3}}{f^*(M, N, h^*)} dr \right]^{-1}$$

The linear dynamic stiffness coefficient can be obtained by evaluating the partial derivative of film force with respect to the minimum film thickness and then taking the value under steady state.

$$S^* = - \frac{72\pi}{M^2 f^{*2}(M, N, h^*)} \left[1 - \frac{\beta_1^2}{(\beta_1^2 - \beta_2^2)} \sec^2 h(0.5\beta_2 h^*) + \frac{\beta_2^2}{(\beta_1^2 - \beta_2^2)} \sec^2 h(0.5\beta_1 h^*) \right] \int_{r^*=0}^1 r^{*3} dr$$

Similarly, the linear dynamic damping coefficient can be obtained by evaluating the partial derivative of film force with respect to the squeezing velocity, and then taking the value under steady state.

$$D^* = \frac{36\pi^2}{\left[\int_{r^*=0}^1 \frac{r^{*3} dr}{f^*(M, N, h^*)} \right]^{-2}}$$

The above integrations are solved by using Gaussian Quadrature Method.

3. RESULTS AND DISCUSSIONS

Figure-2 presents the non-dimensional MHNN dynamic stiffness coefficient as a function of r^* for different values of the Hartmann Number under non-Newtonian parameter of couple stresses $N=0$ under $h_c^*=0.5$ and $k=1$. Figure 3 presents the non-dimensional MHNN dynamic stiffness coefficient as a function of r^* for different values of the Hartmann Number under non-Newtonian parameter of couple stresses $N=0.03$ under $h_c^*=0.5$ and $k=1$. Figure-4 presents the non-dimensional MHNN dynamic stiffness coefficient as a function of r^* for

different values of the Hartmann Number under non-Newtonian parameter of couple stresses $N=0.06$ under $h_c^*=0.5$ and $k=1$. Figure 5 presents the non-dimensional MHNN dynamic stiffness coefficient as a function of r^* for different values of the Hartmann Number under non-Newtonian parameter of couple stresses $N=0.08$ under $h_c^*=0.5$ and $k=1$. Figure 6 presents the non-dimensional MHNN dynamic stiffness coefficient as a function of r^* for different values of the Hartmann Number under non-Newtonian parameter of couple stresses $N=0.1$ under $h_c^*=0.5$ and $k=1$. Bearing stiffness coefficients are observed to increase slightly with increasing Hartmann Numbers. Decreasing the porous squeezing film height increases the values of the stiffness coefficient. Totally, the increments in values of the stiffness coefficients are more pronounced for porous squeeze film MHNN curved circular plates with a smaller squeezing film height and a larger Hartmann number. Comparing with the Newtonian film, higher stiffness coefficients are obtained for MHNN porous curved circular plates with the application of magnetic fields. Generally, the MHNN porous curved circular plates provide a significant improvement in dynamic stiffness characteristics, especially for a larger value of the Hartmann number.

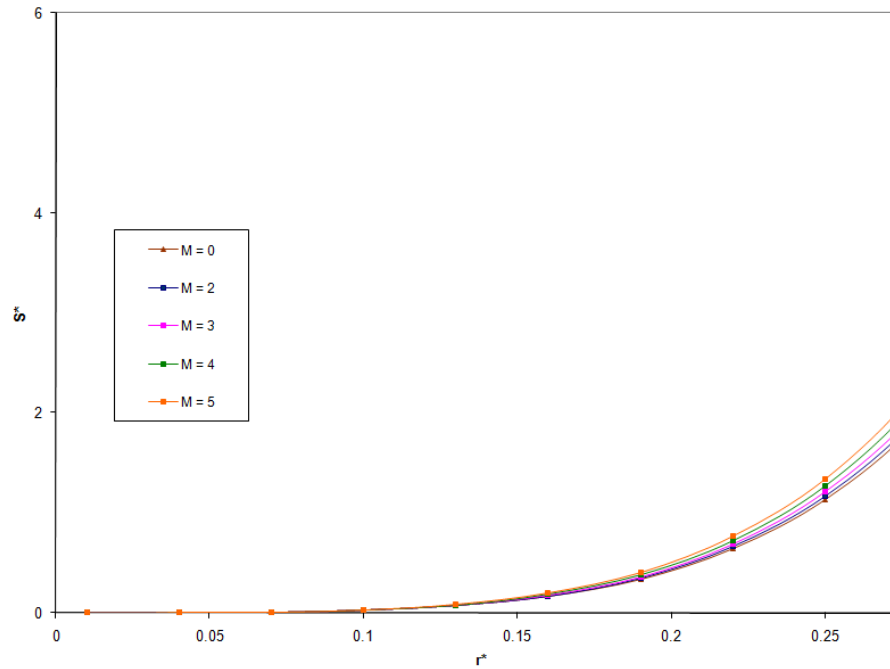
www.arpnjournals.com

Figure-2. MHNN dynamic stiffness coefficient as a function of r^* for different values of the Hartmann Number under non-Newtonian parameter of couple stresses $N=0$

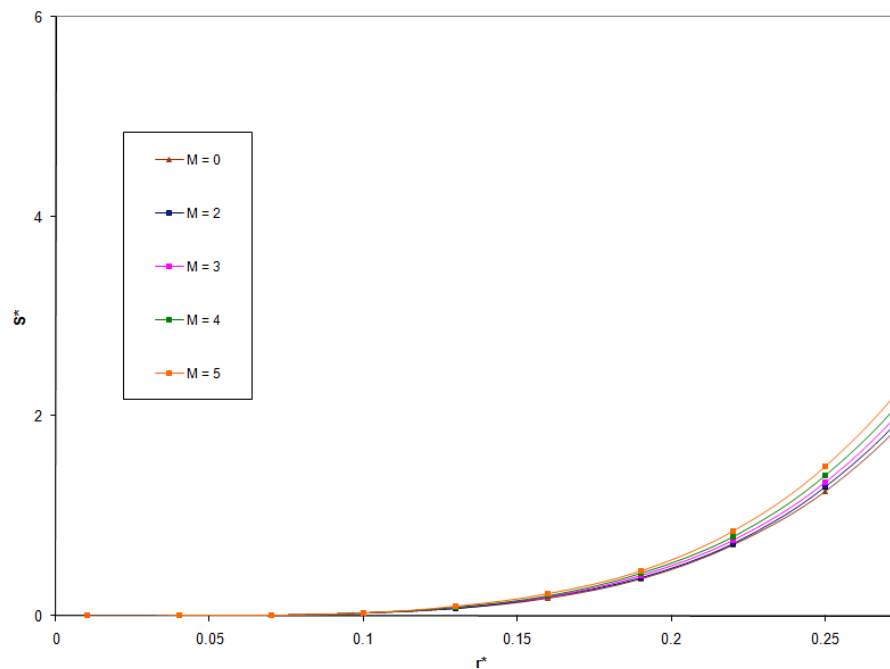


Figure-3. MHNN dynamic stiffness coefficient as a function of r^* for different values of the Hartmann Number under non-Newtonian parameter of couple stresses $N=0.03$.



www.arnjournals.com

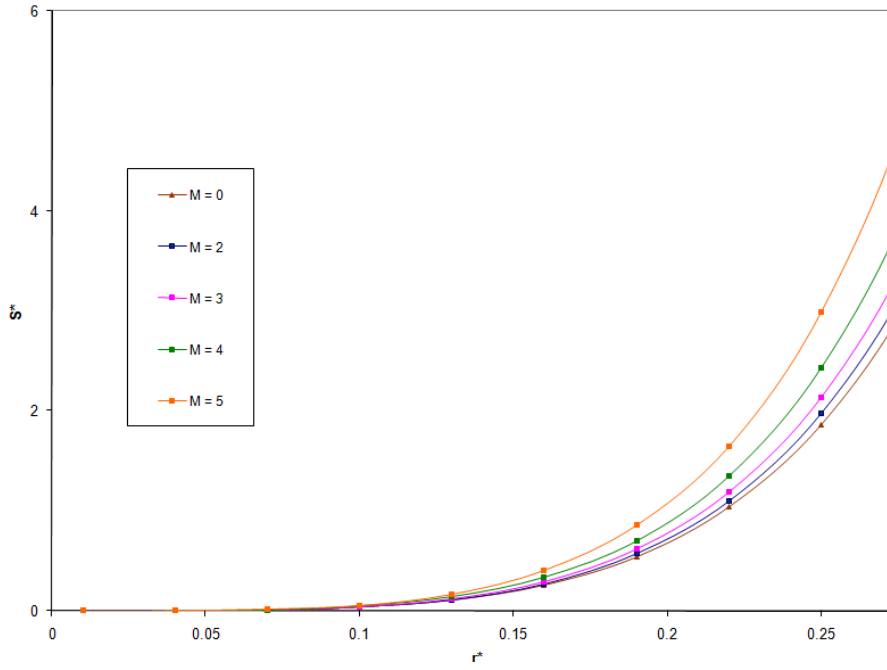


Figure-4. MHNN dynamic stiffness coefficient as a function of r^* for different values of the Hartmann Number under non-Newtonian parameter of couple stresses $N=0.06$.

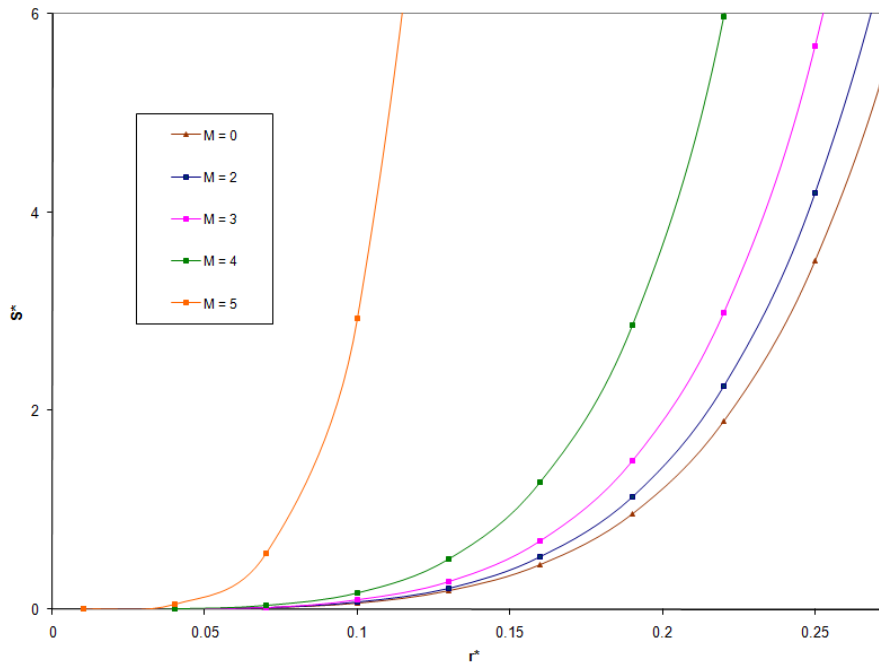


Figure-5. MHNN dynamic stiffness coefficient as a function of r^* for different values of the Hartmann Number under non-Newtonian parameter of couple stresses $N=0.08$.

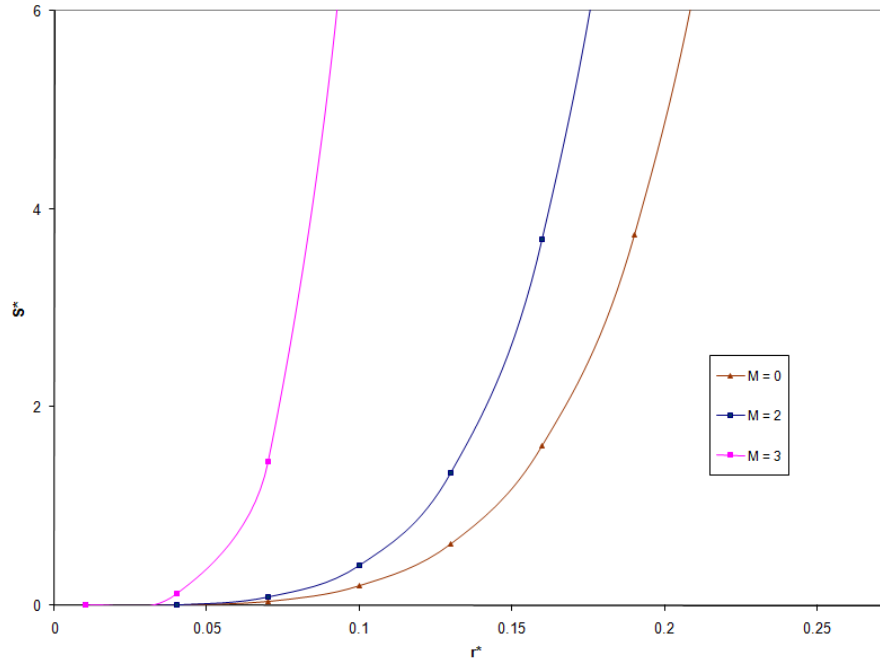


Figure-6. MHNN dynamic stiffness coefficient as a function of r^* for different values of the Hartmann Number under non-Newtonian parameter of couple stresses $N=0.1$

Figure-7 presents the non-dimensional MHNN dynamic damping coefficient as a function of r^* for different values of the Hartmann Number under non-Newtonian parameter of couple stresses $N=0$ under $h_c^*=0.5$ and $k=1$. Figure-8 presents the non-dimensional MHNN dynamic damping coefficient as a function of r^* for different values of the Hartmann Number under non-Newtonian parameter of couple stresses $N=0.03$ under $h_c^*=0.5$ and $k=1$. Figure-9 presents the non-dimensional MHNN dynamic damping coefficient as a function of r^* for different values of the Hartmann Number under non-Newtonian parameter of couple stresses $N=0.06$ under $h_c^*=0.5$ and $k=1$. Figure-10 presents the non-dimensional MHNN dynamic damping coefficient as a function of r^* for different values of the Hartmann Number under non-Newtonian parameter of couple stresses $N=0.08$ under $h_c^*=0.5$ and $k=1$. Figure-11 presents the non-dimensional MHNN dynamic damping coefficient as a function of r^* for

different values of the Hartmann Number under non-Newtonian parameter of couple stresses $N=0.1$ under $h_c^*=0.5$ and $k=1$. Damping coefficients are observed to increase with increasing values of the Hartmann numbers. Decreasing the squeezing film height increases the values of the damping coefficients. It is observed that the increments in values of the damping coefficients are more pronounced for MHNN porous curved circular plates with smaller squeezing film heights and larger Hartmann numbers. Comparing with Newtonian case, the MHNN porous curved circular plates signifies an increase in values of the damping coefficients by the externally applied magnetic fields. On the whole, the effects of applied magnetic fields on the dynamic damping characteristics are more pronounced for the MHNN porous curved circular plates operating at a larger Hartmann number.

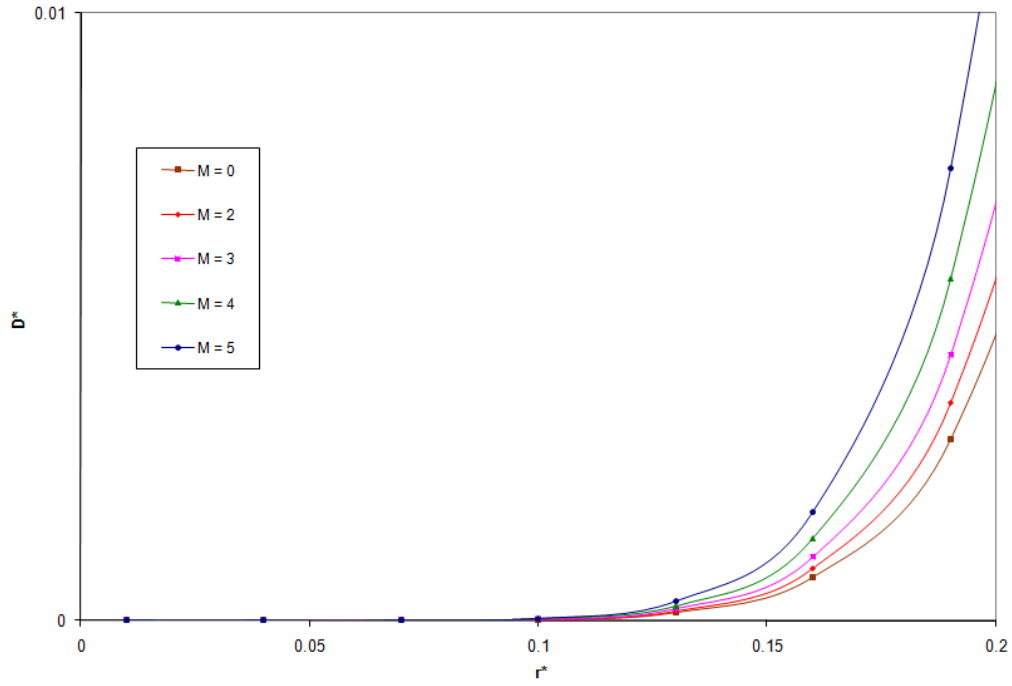


Figure-7. MHNN dynamic damping coefficient as a function of r^* for different values of the Hartmann Number under non-Newtonian parameter of couple stresses $N=0.001$.

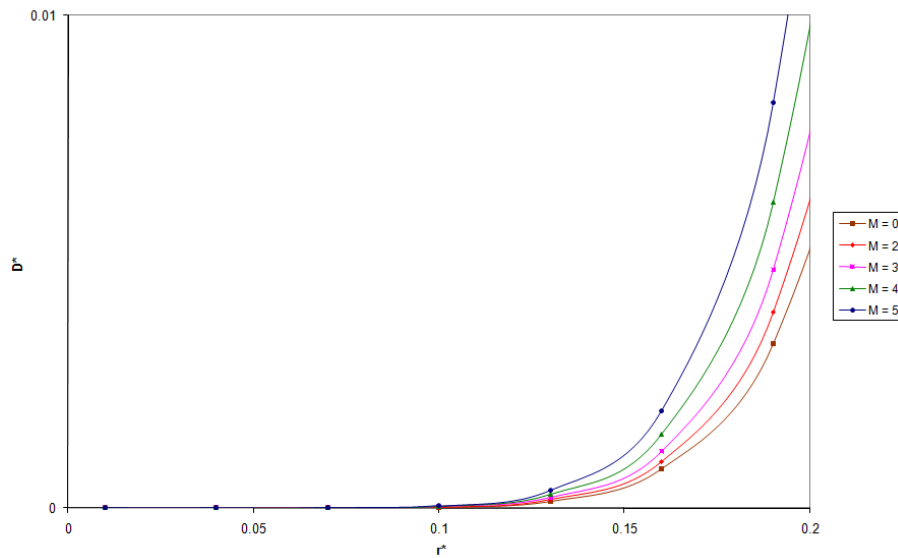


Figure-8. MHNN dynamic damping coefficient as a function of r^* for different values of the Hartmann Number under non-Newtonian parameter of couple stresses $N=0.03$.

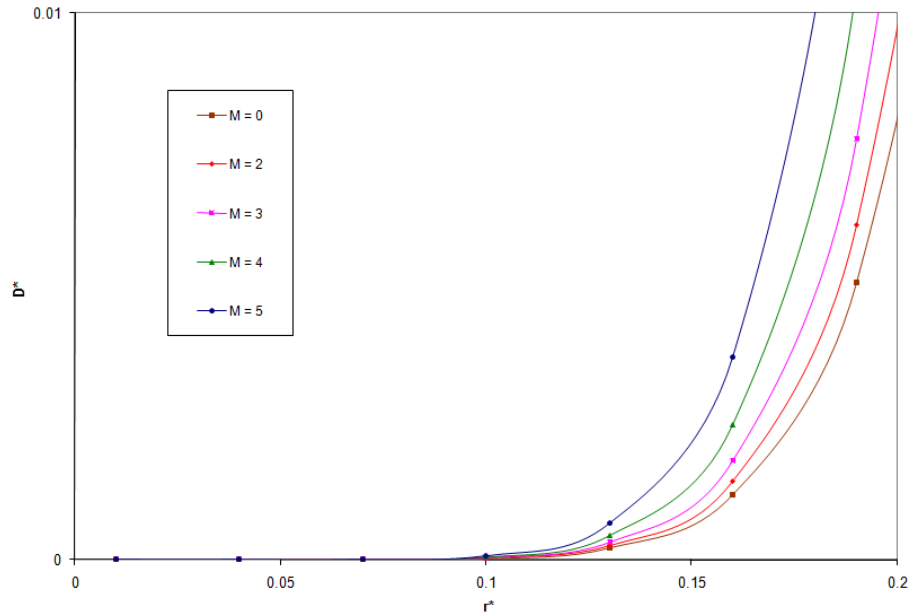


Figure-9. MHNN dynamic damping coefficient as a function of r^* for different values of the Hartmann Number under non-Newtonian parameter of couple stresses $N=0.06$.

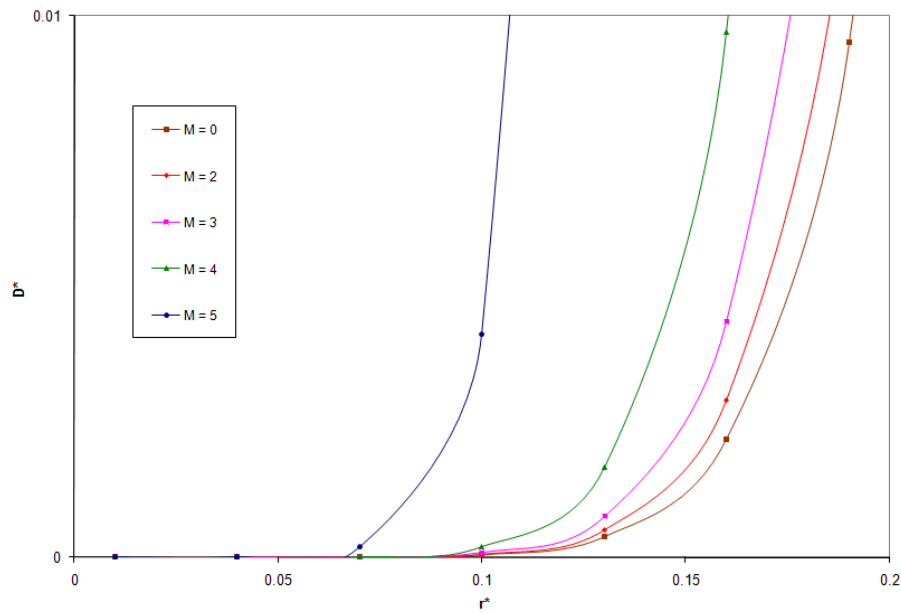


Figure-10. MHNN dynamic damping coefficient as a function of r^* for different values of the Hartmann Number under non-Newtonian parameter of couple stresses $N=0.08$.

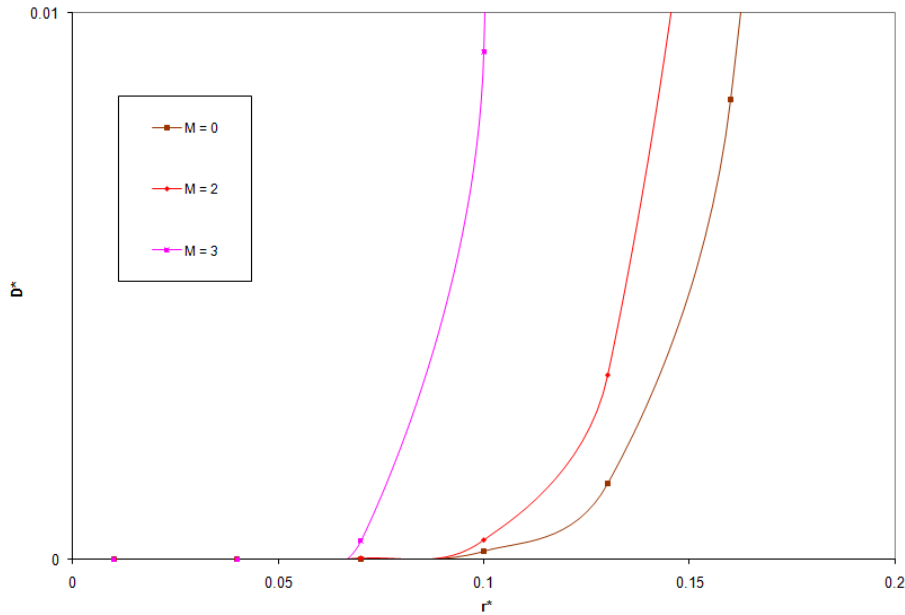


Figure-11. MHNN dynamic damping coefficient as a function of r^* for different values of the Hartmann Number under non-Newtonian parameter of couple stresses $N=0.1$

Table-1. Comparison of the Porous MHNN Stiffness coefficient S^* and the Damping coefficient D^* with the Newtonian results under $h_c^*=0.5, k=1$ and $N = 0$.

r^*	Newtonian results Murthi [8]		Present study: Porous squeeze film MHNN curved circular plates					
			$M = 0$		$M = 2$		$M = 5$	
	S^*	D^*	S^*	D^*	S^*	D^*	S^*	D^*
$r^*=0.13$	0.069077	0.000128	0.069077	0.000128	0.071300	0.000154	0.083069	0.000328
$r^*=0.16$	0.164117	0.000711	0.164117	0.000711	0.169308	0.000852	0.196784	0.001797
$r^*=0.22$	0.642647	0.010416	0.642647	0.010416	0.662068	0.012386	0.764836	0.025463

Table-2. Comparison of the Porous MHNN Stiffness coefficient S^* and the Damping coefficient D^* with the Newtonian results under $h_c^*=0.5, k=1$ and $N = 0.03$.

r^*	Newtonian results Murthi [8]		Present study: Porous squeeze film MHNN curved circular plates					
			$M = 0$		$M = 2$		$M = 5$	
	S^*	D^*	S^*	D^*	S^*	D^*	S^*	D^*
$r^*=0.13$	0.075413	0.0001420	0.075413	0.0001420	0.077918	0.000170	0.091480	0.000361
$r^*=0.16$	0.179474	0.0007890	0.179474	0.0007890	0.185340	0.000943	0.217108	0.001982
$r^*=0.22$	0.706014	0.0116270	0.706014	0.0116270	0.728142	0.013783	0.848055	0.028242



Table-3. Comparison of the Porous MHNN Stiffness coefficient S^* and the Damping coefficient D^* with the Newtonian results under $h_c^*=0.5, k=1$ and $N = 0.06$.

r^*	Newtonian results Murti [8]		Present study: Porous squeeze film MHNN curved circular plates					
			$M = 0$		$M = 2$		$M = 5$	
	S^*	D^*	S^*	D^*	S^*	D^*	S^*	D^*
$r^*=0.13$	0.107391	0.000212	0.107391	0.000212	0.138050	0.000257	0.168365	0.000667
$r^*=0.16$	0.257693	0.001188	0.257693	0.001188	0.273120	0.001440	0.406005	0.003717
$r^*=0.22$	1.037004	0.017947	1.037004	0.017947	1.099493	0.021621	1.150238	0.055197

Table-4. Comparison of the Porous MHNN Stiffness coefficient S^* and the Damping coefficient D^* with the Newtonian results under $h_c^*=0.5, k=1$ and $N = 0.08$.

r^*	Newtonian results Murti [8]		Present study: Porous squeeze film MHNN curved circular plates					
			$M = 0$		$M = 2$		$M = 5$	
	S^*	D^*	S^*	D^*	S^*	D^*	S^*	D^*
$r^*=0.13$	0.183823	0.000382	0.183823	0.000382	0.214864	0.000507	11.63171	0.047038
$r^*=0.16$	0.448516	0.002180	0.448516	0.002180	0.526226	0.002896	44.27433	0.414605
$r^*=0.22$	1.892079	0.034607	1.892079	0.034607	2.244465	0.046197	238.1474	81.86609

Table-5. Comparison of the Porous MHNN Stiffness coefficient S^* and the Damping coefficient D^* with the Newtonian results under $h_c^*=0.5, k=1$ and $N = 0.1$.

r^*	Newtonian results Murti [8]		Present study: Porous squeeze film MHNN curved circular plates					
			$M = 0$		$M = 2$		$M = 5$	
	S^*	D^*	S^*	D^*	S^*	D^*	S^*	D^*
$r^*=0.13$	0.618179	0.001382	0.618179	0.001382	1.337763	0.003370	57.30593	0.1663822
$r^*=0.16$	1.605775	0.008415	1.605775	0.008415	3.695042	0.021768	78.12621	5.294420
$r^*=0.22$	8.210355	0.162688	8.210355	0.162688	23.44964	0.519522	380.757	96.54626

The dynamic squeeze film characteristics for porous curved circular plates are improved by the use of an electrically conducting non-Newtonian fluid in the presence of external magnetic fields as compared to the case of Newtonian squeeze film results of Murti [8] are illustrated in the Table 1 to Table 5. Table values illustrate the MHNN Stiffness Coefficient and the MHNN Damping Coefficient of porous curved circular squeeze films are improved for higher values of magnetic Hartmann Number M .

4. CONCLUSIONS

Comparing with the conventional Newtonian case, the MHNN curved circular porous squeeze film dynamic characteristics are improved by the use of an electrically conducting non-Newtonian fluid in the presence of external magnetic fields.

REFERENCES

- [1] Ahmad N and Singh J.P. 2007. A model for couple-stress fluid film mechanism with reference to human joints. Proceedings of the Institution of Mechanical Engineers: Journal of Engineering Tribology. 221: 755-759.
- [2] Elsharkawy A.A. and AL-Fadhalah K.I. 2008. Separation of a sphere from a flat in the presence of couple stress fluids. Lubrication Science. 20: 61-74.
- [3] Hamrock B.J. 1994. Fundamentals of Fluid Film Lubrication, McGraw-Hill. pp. 286-287.
- [4] Lin J.R., Chu L.M. and Lu R.F. 2014. MHNN curved circular squeeze films. Journal of Marine Science and Technology. 22(5): 566-571.



www.arpnjournals.com

- [5] Lin J.R., Lu, R.F. and Liao, W.H. 2004. Analysis of MHD squeeze film characteristics between curved annular plates. *Industrial Lubrication and Tribology*. 56: 300-305.
- [6] Lin J.R. 2010. MHD steady and dynamic characteristics for wide tapered-land slider bearings. *Tribology International*. 43: 2378-2383.
- [7] Malik, M. and Singh D.V. 1980. Analysis of finite MHD journal bearings. *Wear*. 64: 273-280.
- [8] Murti P.R.K. 1975. Squeeze films in curved circular plates. *ASME Journal of Lubrication Technology*. 97: 650-652.
- [9] Oliver D.R. 1988. Load enhancement effects due to polymer thickening in a short model journal bearing. *Journal of Non-Newtonian Fluid Mechanics*. 30: 185-189.
- [10] Stokes V.K. 1966. Couple stresses in fluid. *Physics of Fluids*. 9: 1709-1715.
- [11] Sundarammal K., Ali. J. Chamkha and Santhana Krishnan N. 2014. MHD squeeze film characteristics between finite porous parallel rectangular plates with surface roughness. *International journal of Numerical methods for heat and fluid flow*. 24(7): 1595-1609.
- [12] Santhana Krishnan Narayanan and Sundarammal Kesavan. 2015. Magneto-Hydrodynamics Non-Newtonian Squeeze film characteristics of porous Curved Circular Plates. *ARPJN Journal of Engineering and Applied Sciences*. 10(14): 5895-5907.